Delocalisation in High-Resolution TEM Images of Platinum Catalyst Nanoparticles

L. Cervera Gontard[1], R. Dunin-Borkowski[1], M. Hÿtch[2], D. Ozkaya[3], L.-Y. Chang[4], A. Kirkland[4] and C. Hetherington[4]
1. Department of Materials Science and Metallurgy, Cambridge University, UK 2. Centre National de Recherche Scientifique, Vitry-sur-Seine, France 3. Johnson Matthey Technology Centre, Reading, UK 4. Department of Materials, Oxford University, UK

BIOGRAPHY

Lionel Cervera Gontard studied physics at the University of Seville, Spain , specialising in microelectronics. He then spent two years working in the National Centre for Microelectronics in Seville. He is now finishing his PhD in the Department of Materials Science and Metallurgy at the University of Cambridge on the application and development of advanced transmission electron microscopy techniques for the study of heterogeneous catalyst nanoparticles. His PhD is sponsored by Johnson Matthey.

ABSTRACT

A focus-dependent displacement between the positions in the darkfield and bright field images of small crystalline particles has been noted in the past. Delocalisation is an imaging artifact that can result in the presence of lattice fringes outside a crystal imaged in a transmission electron microscope in the presence of spherical aberration and/or defocus. Here, we show that delocalisation can be used to provide useful information, in the form of the absolute defocus values of catalyst nanoparticles. This information is useful for interpreting images obtained using techniques such as exit wavefunction restoration.

KEYWORDS

high-resolution transmission electron microscopy, brightfield, darkfield, delocalisation, spherical aberration, focus, catalyst nanoparticles

ACKNOWLEDGEMENTS

The authors are grateful to Peter Ash, Greg Goodlet, Tim Hyde, Steve Spratt and David Thompsett from Johnson Matthey for useful discussions.

AUTHOR DETAILS

Lionel Cervera Gontard, Department of Materials Science and Metallurgy, University of Cambridge, Pembroke Street, Cambridge CB2 3QZ, UK
Tel: +44 (0) 1223 334597
E-mail: lc358@cam.ac.uk

Microscopy and Analysis 20(6):5-7 (UK), 2006

INTRODUCTION

Most industrial heterogeneous catalysts comprise high-surface-area solids, onto which an active component is dispersed in the form of very small particles. The preparation of commercial catalysts is generally not well controlled, and is often based on accumulated experience. Transmission electron microscopy (TEM) is a key experimental tool for the characterisation of catalyst nanoparticles with atomic resolution [1].

The high spatial and temporal coherence of a field emission gun (FEG) TEM increase the information limit of the microscope. However, at large defocus values, the contrast transfer function of the microscope contains many oscillations, which lead to contrast reversals and delocalisation of the information in the image. Detail in the image is then displaced by an amount that increases with defocus [2]. Although the use of aberration correctors on modern TEMs [3,4] has improved the interpretable resolutions of images, comparisons with simulations are still required to understand the observed contrast.

There is great benefit in combining the information that is present in a defocus series of images, in effect extending the point resolution of the microscope to the information limit [5,6]. Figure 1 shows the result of using such an approach to image a Pt catalyst nanoparticle [7]. Both the surface atomic arrangement of the Pt particle and details of its graphitic carbon support can be seen in this image. Although TEM images can now be used to provide sub-Ångstrom resolution information about materials, in this article we are interested primarily in the additional information that can be obtained as a result of the presence of objective lens aberrations. It has long been known that displacements between bright-field and dark-field images can be used to measure certain imaging parameters of the objective lens of a microscope [8].

Here, we show that delocalisation in HRTEM images can be used to extract useful information about a specimen and about the imaging conditions, both qualitatively and quantitatively. Our analysis is facilitated by the use of geometrical phase analysis to measure local lattice fringe displacements [9,10].

MATERIALS AND METHODS

We examined Pt nanoparticles, with an average size of 5 nm, which were supplied on a partially graphitised carbon support. This combined system has important industrial applications in fuel cells and car exhausts. The samples, which were in the form of a dry powder, were placed directly onto holey-carbon copper TEM grids.

Experimental images were acquired at 200 kV using a JEOL 2200FS FEG TEM equipped with a spherical aberration corrector, at a nominal magnification of 500k. This instrument, which is located in the Department of Materials in Oxford University (UK), incorporates aberration correctors in both its imaging and its probe-forming lenses, as well as an in-column omega-type energy filter. A double-hexapole system can be used to eliminate aberrations up to the third order. Here, as we

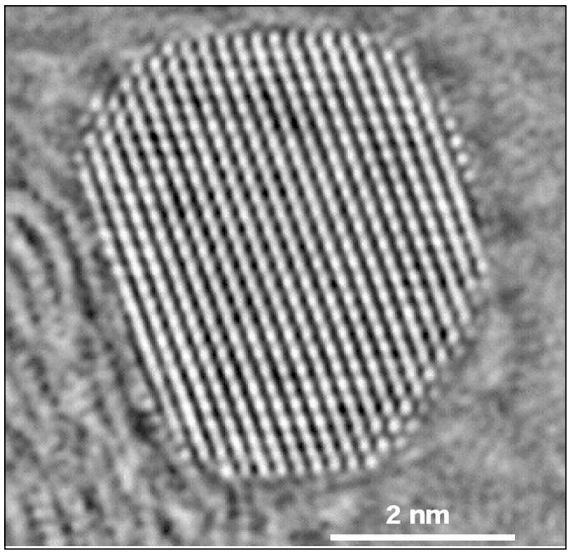

Figure 1:
Focal-series reconstruction of the phase shift of a 5 nm Pt particle supported on graphitic carbon, obtained from a series of 20 images acquired at 200 kV using a defocus step size of 5 nm, with the spherical aberration coefficient C_s adjusted to -30 µm.

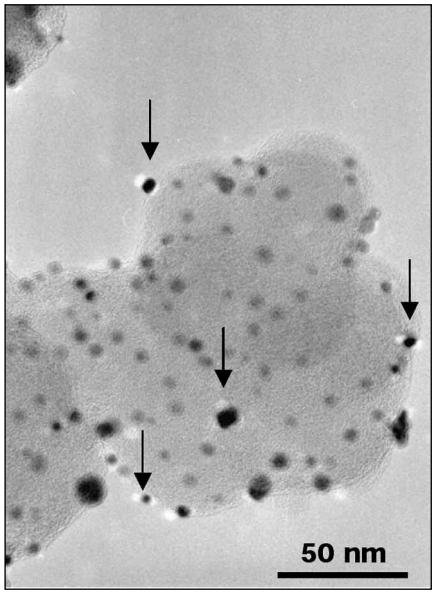

Figure 2:
Low magnification bright-field image of Pt particles on a carbon support showing the effects of delocalisation (arrowed).

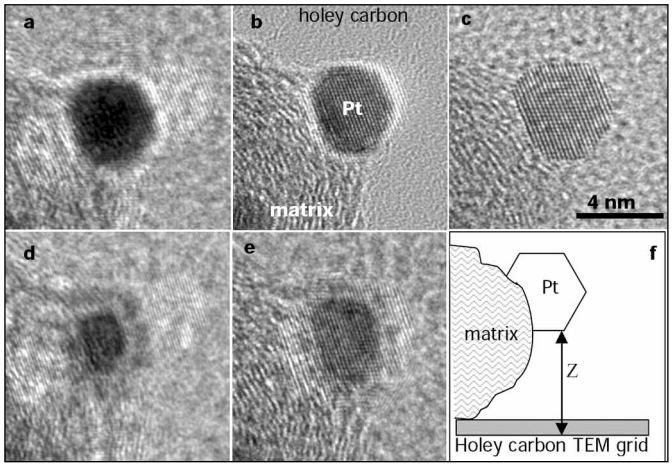

Figure 3:
(a-e) High-resolution lattice images of the Pt particle shown in Figure 1, obtained as a function of defocus at 200 kV using a spherical aberration coefficient C_s of 0.5 mm. The defocus step size between successive images is 100 nm. When the particle is close to focus in (c), delocalisation is minimised. (f) Illustration of the difference in height that is possible between a Pt particle and its holey carbon support film.

are interested in the effects of the aberrations, we acquired images using the uncorrected coefficient of spherical aberration of the objective lens C_s of 0.5 mm (corresponding to 0.19 nm point resolution at Scherzer defocus).

DELOCALISATION OF NANOPARTICLES

The extent of image delocalisation (i.e. the image displacements) depends on the spherical aberration coefficient and on the defocus value used. For a perfectly homogeneous crystal, which has uniform thickness, no defects and translational symmetry, delocalisation effects are not readily apparent. Any imperfection or discontinuity, such as at the edge of a specimen, destroys this translational symmetry locally.

Figure 2 shows a low magnification bright-field defocused image of Pt particles supported on graphitic carbon. Some of the particles are diffracting strongly and are associated with adjacent regions of bright contrast, which results from delocalisation.

Figure 3 shows a defocus series of high-resolution lattice images of a single Pt particle. When imaged out of focus, Fresnel fringes appear around the edge of the particle, and in addition the lattice fringes are displaced with respect to the true position of the particle, which becomes progressively darker with increasing defocus. The displaced lattice fringes move away from the particle approximately linearly with increasing defocus. Despite C_s not being zero, delocalisation is minimised in one of the images (Figure 3c), because in this orientation a single spatial frequency dominates the observed contrast (see below).

QUALITATIVE INFORMATION FROM DELOCALISATION

Qualitatively, the image shifts that are associated with delocalisation can be used to provide information about the orientation of a particle. Figure 4a illustrates the fact that the regions of bright contrast that surround a particle move in specific directions, which are related to its orientation. The angle of 70° observed between the displaced images is close to the value of 70.52° expected between 111-type reflections in a cubic structure oriented close to a [011] zone axis. In Figure 4b, the angle between the reflections is 90° and the fringes have a spacing of 0.19 nm, corresponding to the 200 plane spacing of Pt. The relative intensities of the displaced bright regions depend on the degree and direction of misalignment of the particle from the exact zone axis orientation.

QUANTITATIVE INFORMATION FROM DELOCALISATION

The extent of image delocalisation depends on the spatial frequency **g** and on the wave aberration function of the objective lens $\chi(\mathbf{g})$ [2]. It is large when $|\nabla\chi(\mathbf{g})|$ is large. Neglecting higher order aberrations, the equation that relates the displacement of the image ΔR to the imaging conditions is:

$$\Delta R = |\nabla\chi(\mathbf{g})| = \lambda|\mathbf{g}|\,\Delta f + C_s\lambda^3|\mathbf{g}|^3 \qquad \text{Eq.1}$$

where Δf is the defocus and λ is the electron wavelength.

From Equation 1, it follows that for each spatial frequency in an image ΔR varies linearly with defocus. Figure 5 shows Equation 1 plotted as a function of defocus for lower spatial frequency reflections in Pt, for an accelerating voltage of 200 kV, using values for C_s of both 0.5 mm and -30 µm.

The graphs illustrate the fact that for every spatial frequency there is a defocus value for which delocalisation is exactly zero. However, when C_s is close to zero, it is possible to find a defocus value for which the extent of delocalisation can be minimised for all spatial frequencies at the same time.

ABSOLUTE DEFOCUS MEASUREMENT

The defocus value of an image is usually obtained either by comparing the contrast in the image with simulations or from the analysis of diffractograms acquired from amorphous material close to the area of interest (in this case the holey carbon film on the TEM grid).

However, for a nanoparticle, the defocus obtained from diffractogram analysis of the support film may be very different from the true defocus of the particle, as shown schematically in Figure 3f. A method that can be used to find the absolute defocus value of a nanoparticle is now presented. The approach, which relies on the presence of delocalisation associated with a known spatial frequency, is as follows:

1. A through-focus series of bright-field images of the particle is acquired. 2. The extent of delocalisation for a particular spatial frequency in each image is measured, for example by using geometrical phase analysis (see Figure 6). 3. Defocus values are also mea-

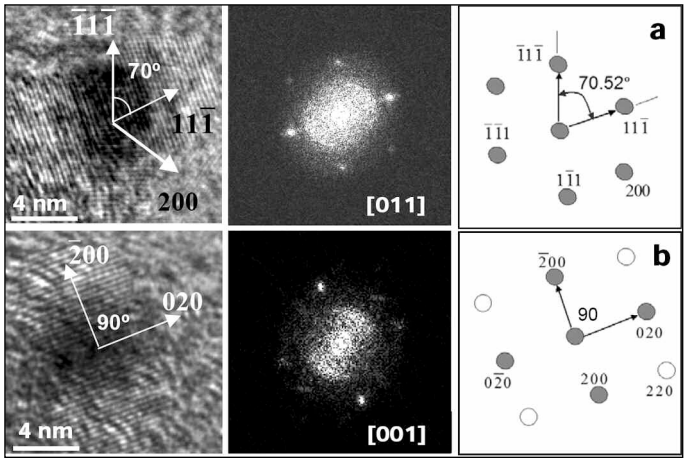

Figure 4:
Illustration of the qualitative use of delocalisation to provide information about the orientation of a nanoparticle. HRTEM images, experimental diffractograms and predicted diffractograms are shown for Pt particles in [011] (a) and [001] (b) orientations.

sured from the support film in each image using diffractogram analysis. 4. The image displacements associated with delocalisation are plotted as a function of the defocus values obtained from diffractogram analysis. 5. The lateral displacement of the graph that is required for consistency with Equation 1 is determined. This value corresponds to the difference in focus between the nanoparticle and the support film (the parameter Z in Figure 3f).

Figure 7 shows the application of this approach to the images of the Pt particle shown in Figure 3. The entire defocus series contained 20 images, with a defocus step size between adjacent images of 100 nm. The slope of the experimental graph matches that predicted using Equation 1 for a spatial frequency that corresponds to the 111 reflection in Pt. The experimental measurements are displaced laterally with respect to the predicted graph by an averaged value of 85 nm. The absolute defocus value of the particle in each image is therefore obtained by subtracting 85 nm from the values measured using diffractogram analysis. According to Equation 1, the slope of the experimental graph shown in Figure 7 can also be used for calibrating the defocus step size if the relevant plane spacing is known. The slight deviation of the experimental slope from the predicted graph in Figure 7 therefore almost certainly results from a small error in the defocus step calibration.

CONCLUSIONS

Delocalisation is an imaging artifact that is present in all transmission electron microscopes. In the absence of spherical aberration, delocalisation is absent at zero defocus for every spatial frequency. However, if spherical aberration is present, delocalisation can only be removed for one spatial frequency at each defocus value. Here, we have shown that delocalisation can be used qualitatively to provide information about the orientation of a nanoparticle. It can also be used to provide quantitative information about the absolute defocus value of a nanoparticle, when combined with diffractogram analysis. This information is useful for the interpretation of results obtained using techniques such as through-focus exit wavefunction restoration.

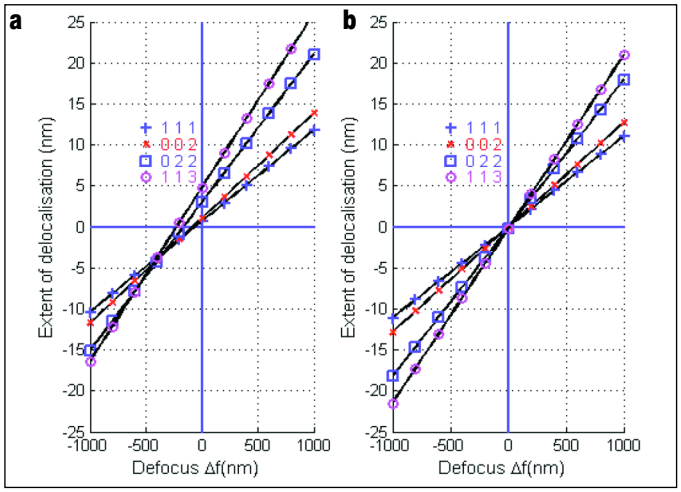

Figure 5:
Theoretical relationship between defocus and the extent of delocalisation (i.e. the image displacement) plotted as a function of spatial frequency for Pt at 200 kV.
(a) C_s = 0.5 mm.
(b) C_s = -30 µm.

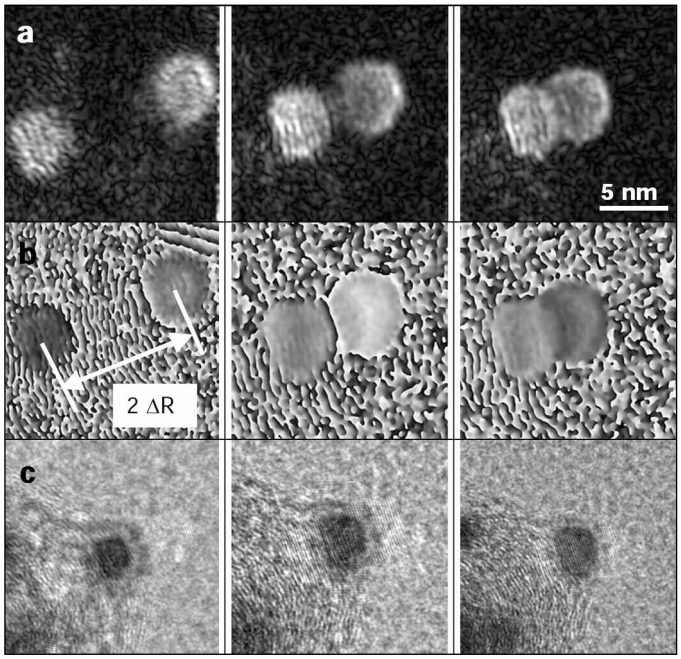

Figure 6:
Amplitude (a) and phase (b) images obtained by applying geometrical phase analysis to the images of a Pt particle shown in (c), for three different defocus values. The amplitude images are more noisy than the phase images and are less useful for determining image displacements.

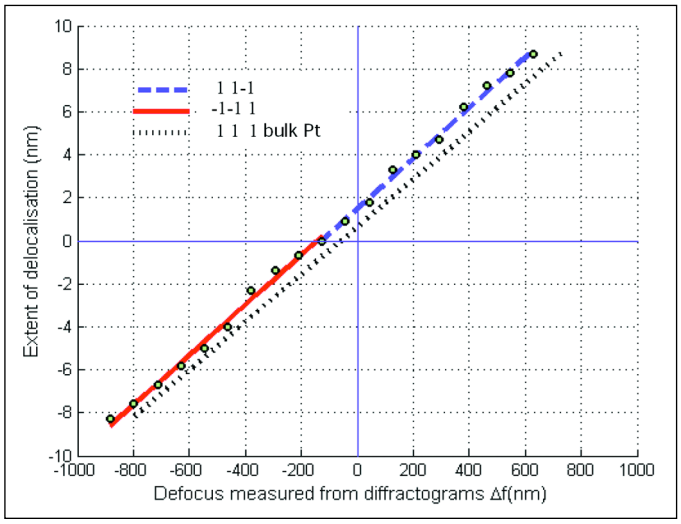

Figure 7:
Dotted line: expected dependence of delocalisation plotted as a function of defocus for the spatial frequency 111 for Pt at 200 kV, for C_s = 0.5 mm. Circles: experimental image displacements plotted as a function of defocus determined from diffractograms. The displacement between the experimental and expected lines provides a measure of the height of the particle from the support film.

1. *Liu, J. Y. Advanced electron microscopy characteris-ation of nanostructured heterogeneous catalysts. Microscopy and Microanalysis 10:55-76, 2004.*
2. *Coene, W. and Jansen, A. J. Image delocalisation and high res-olution tranmission electron microscopic imaging with a field emission gun. Scanning Microscopy Supplement 6:379-403 1992.*
3. *Haider, M. et al. A spherical-aberration-corrected 200kV transmission electron microscope. Ultramicroscopy 75:53-60, 1998.*
4. *Chen, J. H., Zandbergen, H. W. and Van Dyck, D. Atomic imaging in aberration-corrected high-resolution transmission electron microscopy. Ultramicroscopy 98:81-97, 2004.*
5. *Kirkland, A. I., Meyer, R. R. 'Indirect' high-resolution transmission electron microscopy: Aberration measurement and wavefunction reconstruction. Microscopy and Microanalysis 10:401-413, 2004.*
6. *Meyer, R. R. et al. Discrete atom imaging of one-dimensional crystals formed within single-walled carbon nanotubes. Science 289:1324-1326, 2000.*
7. *Cervera Gontard, L., et al. The application of spherical aberration correction and focal series restoration to high-resolution images of platinum nanocatalyst particles. J. Phys. Conference Series 26:25-28, 2006.*
8. *Budinger, T. F., Glaeser, R. M. Measurement of focus and spherical aberration of an electron microscope objective lens. Ultramicroscopy 2:31-41, 1976.*
9. *Hÿtch, M. J. Analysis of variations in structure from high-resolution electron microscopy images by combining real space and Fourier space information. Microscopy Microanalysis Microstructures 8:41-57, 1997.*
10. *Hÿtch, M. J. et al. Measurement of the displacement field of dislocations to 0.03 Å by electron microscopy. Nature 423:270-273, 2003.*

©2006 John Wiley & Sons, Ltd